Taylor & Francis
Taylor & Francis Group

CLINICAL STUDY

◯ OPEN ACCESS ⟳ Check for updates

HYAL1 deficiency attenuates lipopolysaccharide-triggered renal injury and endothelial glycocalyx breakdown in septic AKI in mice

Hongxia Xing[a], Shensen Li[a], Yongchao Fu[a], Xin Wan[b], Annan Zhou[a], Feifei Cao[a], Qing Sun[a], Nana Hu[a], Mengqing Ma[a], Wenwen Li[a] and Changchun Cao[a]

[a]Department of Nephrology, Sir Run Hospital, Nanjing Medical University, Jiangsu, China Nanjing; [b]Department of Nephrology, Nanjing First Hospital, Nanjing Medical University, Jiangsu, China Nanjing

ABSTRACT

Background: Renal dysfunction and disruption of renal endothelial glycocalyx are two important events during septic acute kidney injury (AKI). Here, the role and mechanism of hyaluronidase 1 (HYAL1) in regulating renal injury and renal endothelial glycocalyx breakdown in septic AKI were explored for the first time.

Methods: BALB/c mice were injected with lipopolysaccharide (LPS, 10 mg/kg) to induce AKI. HYAL1 was blocked *in vivo* using lentivirus-mediated short hairpin RNA targeting HYAL1 (LV-sh-HYAL1). Biochemical assays were performed to measure the levels and concentrations of biochemical parameters associated with AKI as well as levels of inflammatory cytokines. Renal pathological lesions were determined by hematoxylin-eosin (HE) staining. Cell apoptosis in the kidney was detected using terminal-deoxynucleoitidyl transferase-mediated nick end labeling (TUNEL) assay. Immunofluorescence and immunohistochemical (IHC) staining assays were used to examine the levels of hyaluronic acid in the kidney. The protein levels of adenosine mono-phosphate-activated protein kinase (AMPK)/mammalian target of rapamycin (mTOR) signaling, endothelial glycocalyx, and autophagy-associated indicators were assessed by western blotting.

Results: The knockdown of HYAL1 in LPS-subjected mice by LV-sh-HYAL1 significantly reduced renal inflammation, oxidative stress, apoptosis and kidney dysfunction in AKI, as well as alleviated renal endothelial glycocalyx disruption by preventing the release of hyaluronic acid to the blood-stream. Additionally, autophagy-related protein analysis indicated that knockdown of HYAL1 significantly enhanced autophagy in LPS mice. Furthermore, the beneficial actions of HYAL1 blockade were closely associated with the AMPK/mTOR signaling.

Conclusion: HYAL1 deficiency attenuates LPS-triggered renal injury and endothelial glycocalyx breakdown in septic AKI in mice.

Introduction

Sepsis is a clinical syndrome that responds to infection and is manifested by multiple immune response disorders, organ failure, and systemic inflammation [1]. As a severe complication of sepsis, septic acute kidney injury (AKI) is accompanied by kidney apoptosis, inflammation, and renal hemodynamic abnormalities [2]. Due to the heterogeneity of septic AKI pathological process, renal dialysis and kidney replacement are feasible therapies for the treatment of this disease [3]. However, high medical price and shortage of kidney source are two big obstacles to global healthcare systems [4]. Thus. the treatment and mechanisms of septic AKI still need to be further elucidated.

Lipopolysaccharide (LPS) present in the cell wall of Gram-negative bacteria is a main cause of sepsis [5]. LPS contributes to excessive inflammation and oxidative stress, and subsequent severe kidney dysfunction and renal hypoperfusion [6]. Thus, injection LPS into animals has been widely used for establishment of *in vivo* septic AKI models [7].

As the barrier between endothelium and blood plasma, endothelial glycocalyx is located on the side of endodermal lumen and exerts crucial functions in mediating vascular permeability [8]. Plasma-related proteins, glycosaminoglycans, proteoglycans and glycoproteins are the main components of glycocalyx [9]. Hyaluronic acid release and syndecan-1 shedding are two indicators of endothelial glycocalyx degradation [10]. Sepsis

---

contributes to endothelial glycocalyx degradation which is associated with alternations in vascular permeability [11]. Recent studies have disclosed the association of impaired microcirculation with renal endothelial glycocalyx in septic AKI [12]. The disruption of endothelial glycocalyx is a process mediated actively by hyaluronidase (hyaluronic acid) and heparanase (two cleavage enzymes), during which the soluble components (e.g., syndecan-1 and hyaluronic acid) of endothelial glycocalyx are released into the bloodstream [13]. To date, several strategies have been proposed to protect against endothelial glycocalyx degradation [14]. However, no clinical therapies for completely protecting or repairing endothelial glycocalyx has yet succeeded [15].

As a member of glycosaminoglycans, hyaluronan (HA, hyaluronic acid) is the main component of the extracellular matrix [16]. HA is primarily distributed in of renal inner papilla interstitium with low HA content in renal cortex [17]. Increases papillary HA attenuates water reabsorption by altering interstitium permeability, suggesting HA can modulate renal fluid balance [18,19]. Hyaluronidases (HYALs) are a kind of enzymes that can degrade HA [20]. HYAL genes contains six members (perm-specific PH-20.13-15, HYAL1/2/3/4 and HYAL-P1, among which HYAL1/2 are the two most characteristic HYAL genes with diverse catalytic properties [21]. Notably, depletion of HYAL1 enhances the accumulation of HA and aggravates inflammation, fibrosis tubular injury in the post-ischemic kidney [22]. However, whether and how HYAL1 can mediate renal function in septic AKI need further exploration.

Autophagy is necessary to mediate stress responses and maintain cellular homeostasis [23]. During autophagy-mediated degradation process, autophagosomes encase stimuli including dysfunctional organelles, long-lived or damaged proteins and intracellular pathogens and subsequently lysosomes eliminate these stimuli [24]. The mTOR signaling can negatively regulate autophagy and the AMPK signaling can promote autophagy *via* restraining the phosphorylation of mTOR [25]. Increasing studies have substantiated the participation of AMPK/mTOR-mediated autophagy signaling in diverse renal injury models [26–28]. However, it is unknown whether the mechanism how HYAL1 protects the kidney is associated with autophagy.

In this study, mice were injected with LPS to establish *in vivo* septic AKI models. First, we explored the role of HYAL1 in mediating renal injury in septic AKI mice. We hypothesized that HYAL1 may disrupt renal endothelial glycocalyx and inhibit autophagy by modulating the AMPK/mTOR signaling in LPS-induced AKI mice. To test our hypothesis, we here designed a series of experiments. Our study illustrates a new mechanism of septic AKI progression, providing novel insights for the treatment of this disease.

Materials and methods

Animals and groups

Forty healthy BALB/c mice at the age of six to eight-weeks (weighing 20–25 g g) were purchased from the Vital River Laboratory Animal Technology Co. Ltd. (Beijing, China). Mice were housed in an air-conditioned environment with a 12 h:12 h light-dark cycle. The experiment was conducted under the approval of the Institutional Ethics Review Committee of Nanjing First Hospital, Nanjing Medical University. Glycocalyx degradation is a process which is actively mediated by cleavage enzymes [13]. Here, we examined the effect of hyaluronidase on glycocalys degradation in AKI by conducting the interference treatment. Lentivirus-mediated short hairpin RNA targeting HYAL1 (LV-sh-HYAL1) and LV-sh-NC were obtained from Genechem (Shanghai, China). We injected LV-sh-HYAL1 or LV-sh-NC into the tail vein one week before LPS injection. These mice were divided into four groups ($n = 10$/group): the LV-NC-treated control mice that received vehicle (Sham + LV-NC); the LV-sh-HYAL1-treated mice that received vehicle (Sham + LV-sh-HYAL1); the LV-NC-treated control mice that received an intraperitoneal injection of 10 mg/kg LPS (LPS + LV-NC); and the LV-sh-HYAL1-treated control mice that received an intraperitoneal injection of 10 mg/kg LPS (LPS + LV-sh-HYAL1). For establishment of septic AKI mice model, the mice in the LPS groups were injected intraperitoneally with 10 mg/kg LPS (Sigma-Aldrich, USA) and the sham group received equivalent dose of normal saline once by intraperitoneal injection [29]. One week before LPS injection, LV-sh-HYAL1 (5×10^7 TU/mouse) were injected intravenously into the tails of Sham + LV-sh-HYAL1 group and the LPS + LV-sh-HYAL1 group [30]. Mice in the Sham + LV-NC group and the LPS + LV-NC group received the equivalent amount of LV-sh-NC by tail intravenous injection [30]. After 24 h later [31], animals were anesthetized by injection of pentobarbital sodium (1%, 40 mg/kg, i.p.), and kidney, urine, and blood samples were collected for subsequent experiments.

Reverse transcriptase quantitative polymerase chain reaction (RT-qPCR)

Total RNAs isolated from murine renal tissues were extracted using TRIzol reagent (Invitrogen) and were reverse transcribed to complementary DNA using

reverse transcription cDNA synthesis kit (Vazyme, China). SYBR Green PCR kit (Takara) was used for RT-qPCR analysis in 7900HT Fast Real-Time PCR System (Applied Biosystems). Inducible nitric oxide synthase (iNOS) level was calculated by the $2^{-\Delta\Delta Ct}$ method [32], and was normalized to GAPDH expression.

Western blotting

Radio-immunoprecipitation assay lysis buffer (Beyotime) was used to extract proteins from murine renal tissues. A BCA assay kit (Beyotime) was used to quantify the obtained proteins. Based on sodium dodecyl sulfate-polyacrylamide gel electrophoresis, proteins were transferred onto polyvinylidene difluoride membranes, and then incubated with primary antibodies including anti-heparanase-1 (ab288438; 1:1000), anti-syndecan-1 (ab128936; 1:1000), anti-p-AMPK (ab133448; 1:1000), anti-AMPK (ab32047; 1:1000), anti-p-mTOR (ab109268; 1:1000), anti-mTOR (ab134903, 1:10000), anti-LC3-I (ab62721; 1:1000), anti-LC3-II (ab192890; 1:2000), anti-p62 (ab109012; 1:10000) and GAPDH (ab8245; 1:500) at 4 °C overnight and subsequently with horseradish peroxidase-labeled IgG (ab6721; 1:1000) secondary antibody at room temperature for 2 h. All antibodies were purchased from Abcam. Protein bands were visualized by BeyoECL Plus (Beyotime) and analyzed using sodium Image Lab 3.0 (Invitrogen).

Biochemical assays

Blood urea nitrogen (BUN) and serum creatinine (Scr) were detected using commercially available blood BUN and serum Scr detection kits (Changchun Huili Biotech, China) following the manufacturer's protocols. The commercial assay kits (Beyotime, Shanghai, China) were used to determine superoxide dismutase (SOD) activity and malondialdehyde (MDA) value. The concentrations of kidney injury molecular-1 (KIM-1) and neutrophil gelatinase-associated lipocalin (NGAL) in urine were measured using ELISA kits (ab213477 and ab199083) following the manufacturer's protocols. Hyaluronidase activity was assessed by an ELISA kit (Echelon Biosciences, USA). The serum TNF-α, IL-1β, and IL-6 levels were assessed using the ELISA kits (Abcam) as per the instructions of respective manufacturer.

Hematoxylin-eosin (HE) staining

Renal sections were subjected to HE staining under a light microscope as previously described methods [33]. Finally, the sections were observed under an optical microscope (Olympus, Tokyo, Japan) at 200× magnification. Tubular necrosis score was calculated using the reported methods [34]. Briefly, 10 none overlapping fields (200×) were randomly selected. The score was obtained by evaluating the degree of cell necrosis, tubule dilatation, cast formation, and loss of brush border in the tubules as follows: 0 refers to none, 1 refers to ≤10%, 2 refers to 11–25%, 3 refers to 26–45%, 4 refers to 46–75%, and 5 refers to >76%.

Terminal-deoxynucleoitidyl transferase-mediated nick end labeling (TUNEL)

According to the manufacturer's instructions, a TUNEL assay kit (Roche Diagnostics, Indianapolis, USA) was used to assess apoptosis in kidney tissues. In five randomly selected fields, the TUNEL-positive cells were counted under microscopy, and the percentage of TUNEL-positive cells was calculated as previously described [35].

Measurement of ROS levels

Dihydroethidium (DHE) fluorescent probe (Sigma-Aldrich) was utilized to evaluate the renal ROS levels following the previously reported protocol [36]. Briefly, the frozen sections were stained with DHE (50 uM) for 30 min at 37 °C. After three washing in PBS, the images of renal sections were photographed using a fluorescent microscope (TE-2000, Nikon).

Immunohistochemical (IHC) staining

Renal sections (4-μm) were dewaxed with xylene and ethanol and then subjected to antigen retrieval. Then 5% H_2O_2 was used to inactivate endogenous peroxidase activity. Sections were blocked with goat serum solution for 1 h and subsequently reacted with the hyaluronic acid antibody (VECTOR laboratories, CA, USA) overnight at 4 °C. The biotin-conjugated secondary antibody (VECTOR laboratories) was added and incubated for 30 min. After staining with diaminobenzidine, sections were fixed with a mounting solution. Finally, a confocal microscope was used to observe tubular area positive for hyaluronic acid.

Immunofluorescence staining

After antigen retrieval and blocking in a blocking solution, the 4-μm sections were incubated with the hyaluronic acid antibody (abx101090, Abbexa, Wuhan, China) overnight at 4 °C. After washing in PBS, the Cy3-labeled secondary antibody (Proteintech, USA) was added and

incubated for 1 h at 37 °C. Then sections were stained with DAPI. An inverted microscope (TE2000; Nikon) was used to observe fluorescence signals.

Statistical analysis

Data of three independent experiments were analyzed with the SPSS 18.0 program and are presented as the mean ± standard deviation. Statistical comparisons among two groups or multiple groups were estimated by Student's *t*-test or one-way ANOVA followed by Bonferroni' s post hoc test. Survival curves was carried out by Kaplan–Meier method. $p < .05$ was considered statistically significant.

Results

HYAL1 downregulation alleviated renal dysfunction in LPS mice

The survival rate of mice in different groups was evaluated. As Figure 1(A) demonstrated, the survival rate of mice in the Sham groups remained 100% from 0 to

120 h. The survival rate of the LPS + LV-NC group dropped to 90% after LPS injection within 12 h and continued to decline to almost 40% at 120 h after LPS injection (Figure 1(A)). However, HYAL1 depletion significantly mitigated LPS-induced reduction in life span of mice and the survival rate of the LPS + LV-sh-HYAL1 group reached 75% at 120 h (Figure 1(A)). Renal function was assessed by measurement of BUN and SCr in serum, major indicators of the kidney damage [37]. The levels of BUN and SCr in serum in LPS groups was markedly higher than those in the Sham groups, while knockdown of HYAL1 reduced serum BUN and SCr levels in LPS mice (Figure 1(B,C)). Urine NGAL and KIM-1 are two key biomarkers for AKI [38]. LPS treatment contributed to elevation of NGAL and KIM-1 levels in urine, which was reversed by silenced HYAL1 (Figure 1(D,E)).
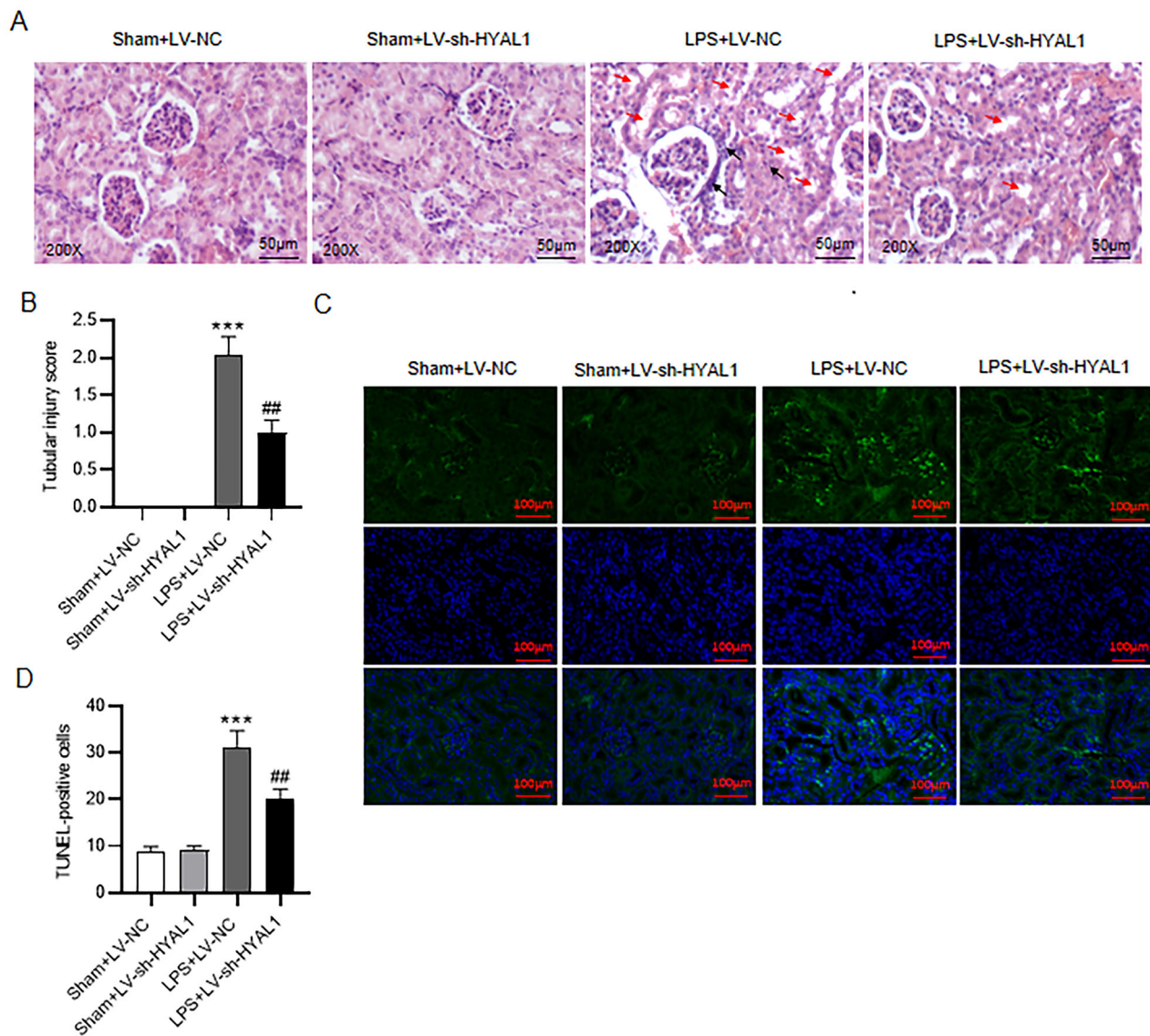
HYAL1 depletion alleviated renal injury of LPS-induced AKI mice

Next, HE staining was performed to show histopathological changes in the kidney. The staining results exhibited alterations in vascular congestion, tubular
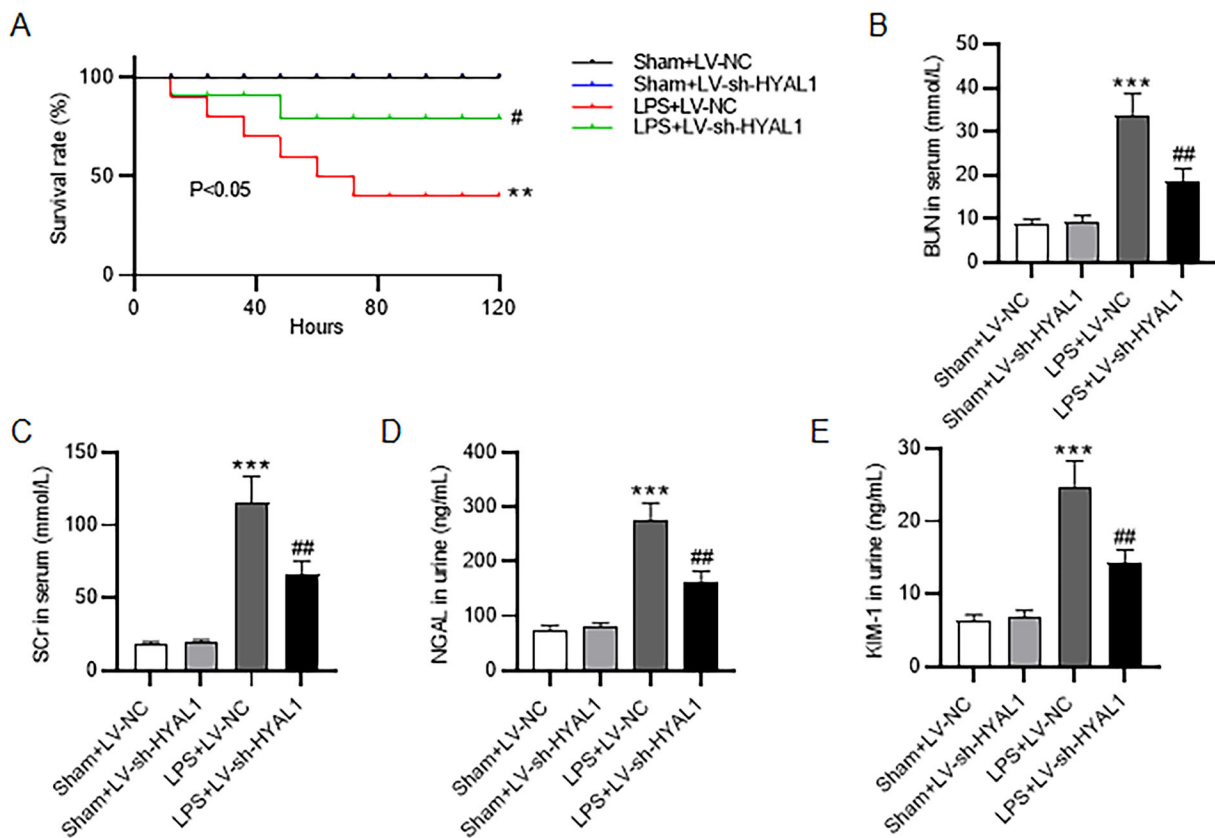
Figure 1. HYAL1 knockdown alleviated renal dysfunction in LPS mice. (A) Survival rates of mice in Sham + LV-NC, Sham + LV-sh-HYAL1, LPS + LV-NC and LPS + LV-sh-HYAL1 groups. (B, C) ELISA for measuring the levels of serum BUN and SCr in Sham + LV-NC, Sham + LV-sh-HYAL1, LPS + LV-NC and LPS + LV-sh-HYAL1 groups. (D, E) ELISA for measuring the levels of NGAL and KIM-1 in urine of mice in Sham + LV-NC, Sham + LV-sh-HYAL1, LPS + LV-NC and LPS + LV-sh-HYAL1 groups. $N = 10$ mice each group. ***$p < .001$ vs. Sham + LV-NC group; ##$p < .01$ vs. LPS + LV-NC group.

Figure 2. HYAL1 depletion alleviated renal injury of LPS-induced AKI mice. (A) HE staining for renal histological changes in Sham + LV-NC, Sham + LV-sh-HYAL1, LPS + LV-NC and LPS + LV-sh-HYAL1 groups (scale bar = 50 μm). 200×. Black arrow presents inflammatory cellular infiltration in the renal interstitium. Red arrow presents severe granular in renal tubular epithelial cells, vacuolar degeneration, and renal tubular necrosis. (B) Tubular injury scores in Sham + LV-NC, Sham + LV-sh-HYAL1, LPS + LV-NC and LPS + LV-sh-HYAL1 groups. (C, D) TUNEL assay for apoptotic cells in renal tissues of mice in Sham + LV-NC, Sham + LV-sh-HYAL1, LPS + LV-NC and LPS + LV-sh-HYAL1 groups (scale bar = 100 μm). $N = 10$ mice each group. ***$p < .001$ vs. Sham + LV-NC group; ##$p < .01$ vs. LPS + LV-NC group.

dilatation, hypercellularity, mesangium expansion, tubular necrosis, and degeneration in mice subjected to LPS. Compared to untreated mice, LV-sh-HYAL1 administration notably reversed these pathological changes. Additionally, the LPS mice had increased inflammatory cellular infiltration in the interstitium. However, LV-sh-HYAL1 significantly attenuated this (Figure 2(A)). Additionally, tubular injury scores in LPS-subjected mice were higher than those in control mice, whereas HYAL1 downregulation reversed LPS-elicited increase in tubular injury scores (Figure 2(B)). Subsequently, TUNEL assay was performed to evaluate cell apoptosis in

kidney tissues. The data revealed that LPS administration stimulated cell apoptosis in kidney tissues compared to the sham group, but this tendency was prevented by HYAL1 knockdown (Figure 2(C,D)).

HYAL1 deficiency inhibited oxidative stress and inflammatory response in LPS mice

LPS-induced AKI disrupts the intracellular redox balance, eliciting oxidative stress [39]. MDA concentration was elevated, and SOD activity was reduced in LPS-treated mice compared with control mice (Figure
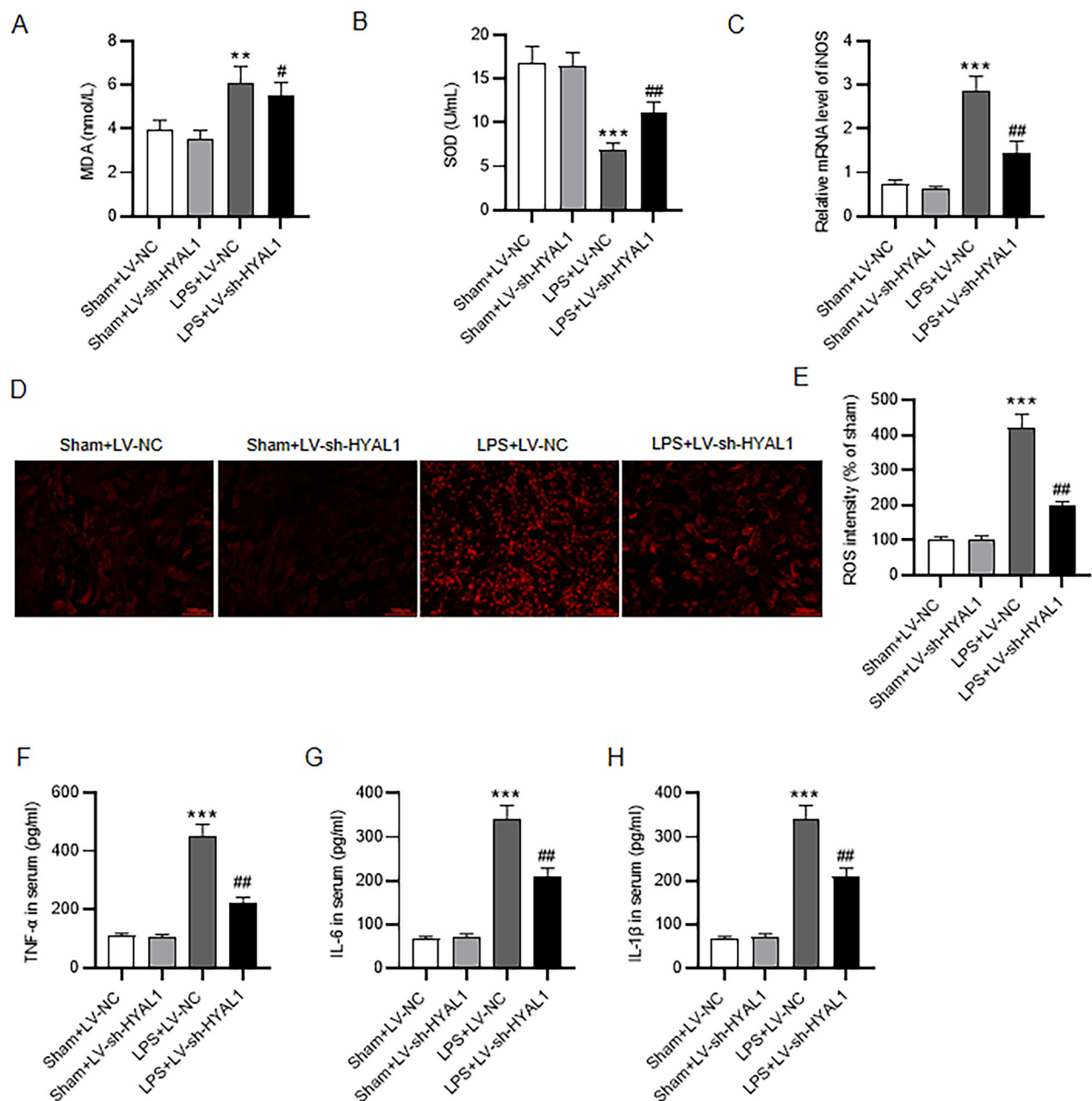
Figure 3. HYAL1 deficiency inhibited oxidative stress and inflammatory response in LPS-induced AKI mice. (A, B) ELISA assay for determining MDA and SOD levels in renal tissues of mice in Sham + LV-NC, Sham + LV-sh-HYAL1, LPS + LV-NC and LPS + LV-sh-HYAL1 groups. (C) RT-qPCR for iNOS mRNA level in renal tissues of mice in Sham + LV-NC, Sham + LV-sh-HYAL1, LPS + LV-NC and LPS + LV-sh-HYAL1 groups. (D) Representative fluorescent images of DHE staining (scale bar = 100 μm). (E) The quantification of the DHE fluorescence intensity. (F–H) ELISA for serum TNF-a, IL-6, and IL-1β levels in Sham + LV-NC, Sham + LV-sh-HYAL1, LPS + LV-NC and LPS + LV-sh-HYAL1 groups. $N = 10$ mice each group. $**p < .01$, $***p < .001$ vs. Sham + LV-NC group; $^{\#}p < .05$, $^{\#\#}p < .01$ vs. LPS + LV-NC group.

3(A,B)). In contrast, LPS-induced increase in MDA level and reduction in SOD level in murine kidneys were neutralized by HYAL1 deficiency (Figure 3(A,B)). We further detected the mRNA level of iNOS using RT-qPCR. LPS stimulation led to upregulation of iNOS mRNA level in murine renal tissues, which was counteracted by depletion of HYAL1 (Figure 3(C)). ROS production was increased in kidney tissues of LPS-treated mice. However, HYAL1 knockdown markedly attenuated LPS-induced renal oxidative stress (Figure 3(D,E)). We next assessed whether inflammation is involved in the actions of HYAL1 knockdown in AKI. The serum TNF-a, IL-6, and IL-1β levels were measured by ELISA. These proinflammatory factors were increased in LPS-treated

mice, and HYAL1 knockdown reduced the release of TNF-a, IL-6, and IL-1β in the serum (Figure 3(F–H)).

HYAL1 knockdown protected endothelial glycocalyx in LPS mice

To assess the endothelial glycocalyx integrity in LPS-induced AKI, the levels of syndecan-1, heparanase-1 and hyaluronic acid as well as hyaluronidase activity were determined. Heparinase-1 is activated in sepsis-AKI and plays a key role in the shedding of endothelial glycocalyx [40]. Syndecan-1 is associated with endothelial glycocalyx skeleton and baseline endothelial dysfunction [41]. Glycocalyx degradation is accompanied by the release of its soluble components into the bloodstream (e.g., syndecan-1 and hyaluronic acid) [10]. As suggested by western blotting, LPS treatment decreased syndecan-1 protein level and increased heparanase-1 protein level in murine renal tissues, which was reversed by silenced HYAL1 (Figure 4(A)). In addition, the LPS group had markedly higher hyaluronidase activity in serum than the Sham group, while HYAL1 knockdown neutralized LPS-caused elevation in hyaluronidase activity (Figure 4(B)). Moreover, LPS stimulation contributed to increase of hyaluronic acid level in murine serum and urine, which was counteracted by HYAL1 deficiency (Figure 4(C,D)). Subsequently, immunofluorescence staining was required for measuring hyaluronic acid level in murine renal endothelial glycocalyx. The results showed that HYAL1 knockdown markedly attenuated the degradation of endothelial glycocalyx (Figure 4(E,F)). IHC staining further revealed that HYAL1 knockdown recovered hyaluronic acid positive tubular area (Figure 4(G,H)), suggesting that HYAL1 knockdown protected endothelial glycocalyx from degradation in LPS mice.

HYAL1 regulated the AMPK/mTOR pathway in LPS mice

To verify the correlation between the actions of HYAL1 knockdown and the AMPK/mTOR pathway, the levels of phosphorylated AMPK (p-AMPK), AMPK, p-mTOR, and mTOR in renal tissues were measured (Figure 5(A)). As western blotting showed, p-AMPK expression was slightly increased while p-mTOR expression was significantly increased after LPS treatment. Interestingly, HYAL1 knockdown reversed these alterations by elevating p-AMPK and downregulating p-mTOR level. It suggested that HYAL1 knockdown inhibited phosphorylation of mTOR by activating AMPK.

HYAL1 deficiency induced autophagy in LPS-induced AKI mice

Since the AMPK/mTOR signaling is closely related to autophagy, we also assessed the protein levels of autophagy-related markers (LC3-II, LC3-I, and p62). As Figure 6(A) illustrated, LPS treatment decreased LC3-II/I ratio and increased p62 protein level in murine renal tissues, suggesting LPS inhibited autophagy in mice. Conversely, HYAL1 depletion counteracted the LPS-induced decrease in LC3-II/I ratio and increase in p62 protein expression, suggesting that HYAL1 knockdown restored autophagy in LPS mice. The schematic presentation of the whole research finding is shown in Figure 7. HYAL1 knockdown enhances autophagy through the AMPK/mTOR pathway to inhibit inflammation and oxidative stress and protect the kidney.

Discussion

Sepsis-induced AKI is hallmarked by severe renal impairment [42]. During the pathogenesis of sepsis, kidney is one of the earliest affected organs [43]. As a classical toll-like receptor 4 agonist, LPS elicits intense inflammation and consequently activates immune system during the process of sepsis [44]. Intraperitoneal injection of LPS into animals is a commonly used *in vivo* model of sepsis [42]. In this study, after LPS administration, the survival rate of mice was significantly reduced. Biochemical analysis and histopathological examination are important methods to evaluate renal function [45]. In our report, LPS-treated mice exhibited obvious renal lesions including tubule dilatation and bleeding, vacuolar degeneration of tubule lining epithelium as well as infiltration of intertubular inflammatory cells. Moreover, our results showed that LPS injection contributed to renal dysfunction of mice evidenced by elevation of serum BUN, SCr, urinary NGAL and KIM-1. All these data indicated that the LPS-induced AKI mouse models were successfully established. We knocked down HYAL1 *via* injecting LV-sh-HYAL1 into LPS-stimulated mice. HYAL1 deficiency counteracted LPS-caused increase in BUN, SCr, NGAL, and KIM-1, showing that HYAL1 knockdown relieved renal dysfunction elicited by LPS in mice. Histopathological examination also demonstrated that downregulation of HYAL1 attenuated LPS-induced renal injury.

HYAL1 is the major hyaluronidase for degradation of hyaluronic acid in somatic tissues [46]. High level of hyaluronic acid has been observed in patients with sepsis [47]. Hyaluronic acid participates in multiple biological processes including cell migration and differentiation [48]. Under some pathophysiological
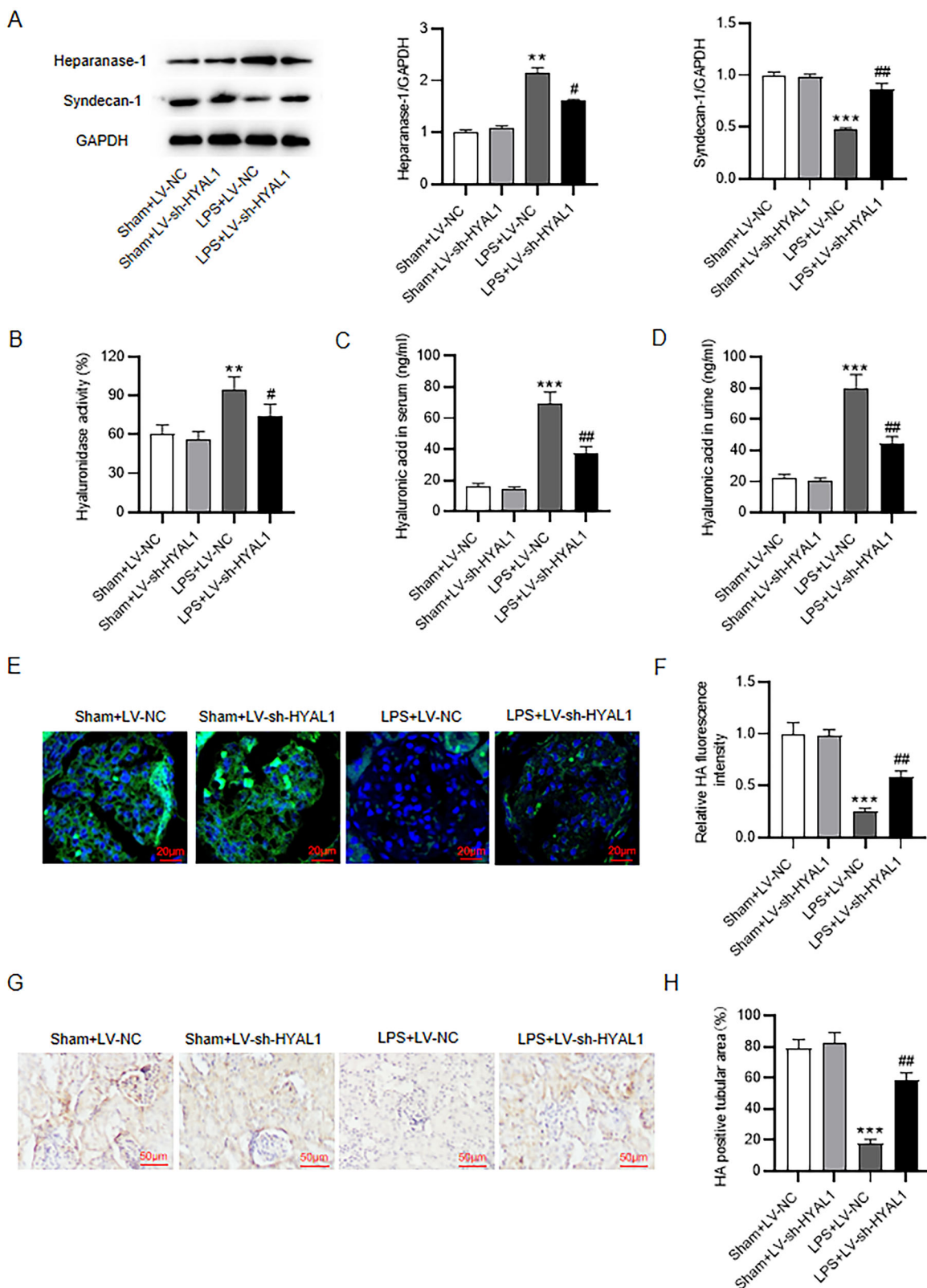
Figure 4. HYAL1 knockdown protected endothelial glycocalyx in LPS-induced AKI mice. (A) Western blotting for syndecan-1 and heparanase-1 protein levels in murine kidneys of Sham + LV-NC, Sham + LV-sh-HYAL1, LPS + LV-NC and LPS + LV-sh-HYAL1 groups. (B) ELISA for hyaluronidase activity in murine serum of Sham + LV-NC, Sham + LV-sh-HYAL1, LPS + LV-NC and LPS + LV-sh-HYAL1 groups. (C, D) ELISA for hyaluronic acid level in murine serum and urine of Sham + LV-NC, Sham + LV-sh-HYAL1, LPS + LV-NC and LPS + LV-sh-HYAL1 groups. (E) Immunofluorescence staining for hyaluronic acid level in murine renal endothelial glycocalyx of Sham + LV-NC, Sham + LV-sh-HYAL1, LPS + LV-NC and LPS + LV-sh-HYAL1 groups (scale bar = 20 μm). (F) The quantification of the hyaluronic acid fluorescence intensity. (G, H) IHC staining for hyaluronic acid level within tubulointerstitial (scale bar = 50 μm). $N = 10$ mice each group. $**p < .01$, $***p < .001$ vs. Sham + LV-NC group; $^{\#}p < .05$, $^{\#\#}p < .01$ vs. LPS + LV-NC group.
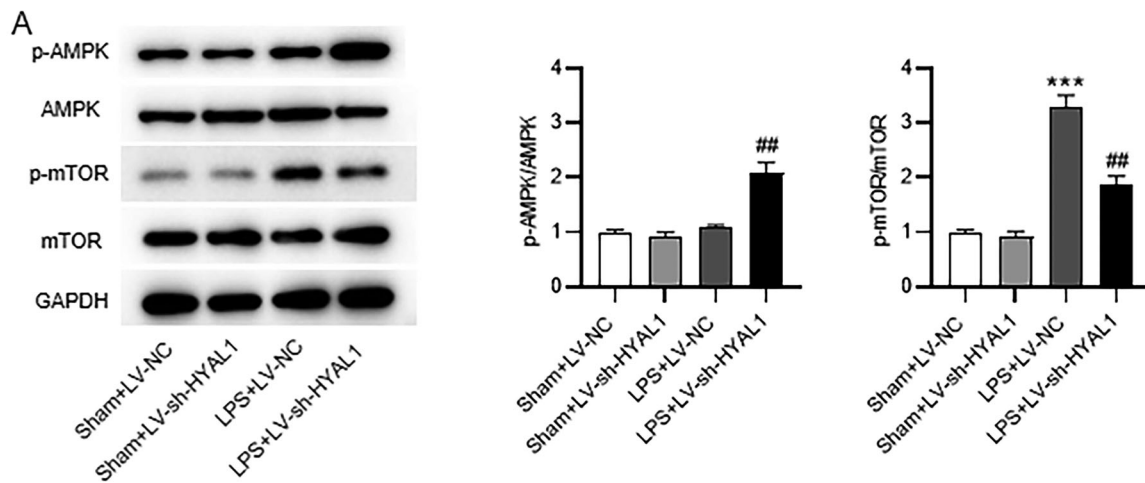
Figure 5. HYAL1 silencing regulated AMPK/mTOP signaling in LPS-induced AKI mice. (A) Western blotting for the protein levels of p-AMPK, AMPK, p-mTOR and mTOR in murine renal tissues of Sham + LV-NC, Sham + LV-sh-HYAL1, LPS + LV-NC and LPS + LV-sh-HYAL1 group. $N = 10$ mice each group. ***$p < .001$ vs. Sham + LV-NC group; ##$p < .01$ vs. LPS + LV-NC group.
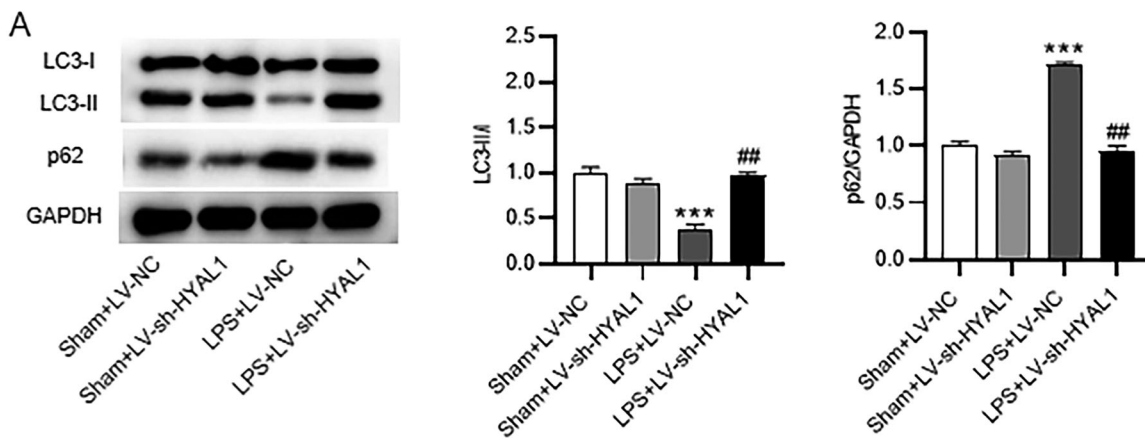
Figure 6. HYAL1 deficiency induced autophagy in LPS-induced AKI mice. (A) Western blotting for the protein levels of LC3-II/I and p62 in murine renal tissues of Sham + LV-NC, Sham + LV-sh-HYAL1, LPS + LV-NC and LPS + LV-sh-HYAL1 groups. $N = 10$ mice each group. ***$p < .001$ vs. Sham + LV-NC group; ##$p < .01$ vs. LPS + LV-NC group.

circumstance, such as diabetic nephropathy [49], allograft rejection [50], and ischemia-reperfusion injury [51], accumulation of hyaluronic acid in the outer medulla and the cortex may accelerate kidney injury. Subsequently, we explored whether HYAL1 exerts its function by regulating hyaluronic acid level in the LPS-induced AKI models. We found HYAL1 downregulation reduced the levels of hyaluronic acid in murine serum and urine. However, a report indicated that deficiency in HYAL1 increased hyaluronic acid accumulation in the post-ischemic kidney and thereby aggravated inflammation and promoted tubular damage [22]. We hypothesized that diverse functions of HYAL1 may be explained by animal models or distinct species. Further studies should be conducted to elucidate the actions of HYAL1 in different conditions.

Oxidative stress is a key factor in regulation of programmed cell death [52,53]. Intracellular antioxidant enzymes (e.g., SOD) play key roles in inhibiting excessive free radical production [54]. During AKI progression, SOD activity is restrained and superoxide generation is accelerated [55]. As the end product of lipid peroxidation, MDA has been reported to be elevated in renal tissues after ischemia/reperfusion (I/R) injury [56] and contribute to increased apoptotic renal cells in AKI [57]. iNOS is an isoform of nitric oxide synthase and iNOS is usually activated in renal tissues under pathological conditions [58]. Suppression of iNOS production has been demonstrated to mitigate oxidative stress and subsequently alleviate I/R induced renal injury [59] and LPS-induced AKI [60]. Mitochondrial ROS induces electron transport chain dysfunction and
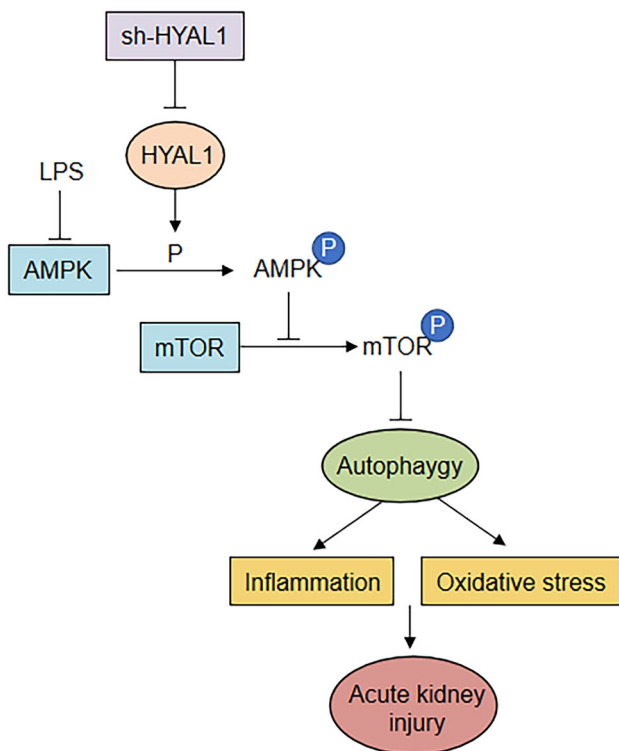
Figure 7. A schematic presentation of the whole research finding. Sepsis-induced AKI is established by intraperitoneally injecting LPS (10 mg/kg) into mice. HYAL1 knockdown enhances autophagy through the AMPK/mTOR pathway to inhibit inflammation and oxidative stress and protect the kidney.

disturbs the balance of energy production [61]. Here, we reported that HYAL1 knockdown attenuated LPS-induced oxidative stress by in septic AKI *in vivo*. Endogenous apoptosis of mitochondrial pathways is activated by various stimuli, including oxidative stress [62]. Here, we confirmed that HYAL1 depletion reversed the promotive impact of LPS stimulation on cell apoptosis of kidneys of mice. Cell survival in response to increased oxidative stress depends on many factors, one of which is nuclear factor erythroid 2-related factor 2 (Nrf2) [63]. Therefore, work in the future should be focused on whether HYAL1 is related to Nrf2/HO-1 signaling pathway-related oxidative stress.

As a protective barrier with delicate latticework structure, glycocalyx is located on the luminal surface of vascular endothelium and exerts protective effects on endothelial cells [64]. Endothelial glycocalyx can inhibit intravascular coagulation and regulate leukocyte migration to maintain the permeability of endothelium [65]. Syndecan (a proteoglycan) and hyaluronan (a glyocosaminoglycan) are essential for maintenance of endothelial glycocalyx integrity [66]. The glycocalyx performs important physiological functions by transmission to the endothelial surface and shielding it from access by cellular components in the bloodstream [67]. Sepsis

resulted in degradation of the endothelial glycocalyx, which is associated with impaired vascular permeability [11]. In our study, injection of LPS contributed to reduction in syndecan-1 level, and elevation of heparanase-1 level, hyaluronidase activity and hyaluronic acid, all of which were offset by silenced HYAL1. Moreover, kidney endothelium glycocalyx layer in the sham-operated mice remained complete and continuous, while the renal capillary glycocalyx of the LPS-treated mice was not continuous with loose and thin structure. Thus, we concluded that deficiency of HYAL1 protected against LPS-induced renal endothelial glycocalyx degradation in septic AKI *in vivo*.

Autophagy is a process of intracellular degradation and fulfills important functions in elimination of dysfunctional organelles [68]. Studies show that activated autophagy can reduce inflammatory cytokines in LPS-induced AKI [69]. The LC3 protein is essential for initiation of autophagosomal membrane formation [70]. The ratio of LC3-II/I level, denoting the conversion of LC3-I to LC3-II, is the key indicator of autophagy [71]. As a selective autophagy adaptor protein, p62 protein expression is contrary to that of LC3 and beclin-1 [72]. The combination of autophagosomes with lysosomes during the degradation process contributes to large consumption of p62 [73]. Therefore, p62 protein accumulation in cells suggests suppression of autophagy [73]. Low autophagy level shown in this study was consistent with the finding of Radovan Vasko's study [74]. LPS treatment contributed to deficiency of autophagy, which led to elevated expression of inflammatory cytokines; perhaps autophagy was destroyed by this dose of LPS. Thus, LPS intervention inhibited autophagy and caused cellular injury. However, knockdown of HYAL1 notably rescued autophagy.

Evidence shows that mTOR is a key negative regulator of autophagy [75]. Additionally, AMPK is able to stimulate autophagy by inhibiting mTOR phosphorylation. Therefore, AMPK/mTOR pathway has been considered an important regulator of autophagy [76]. As previously reported, SIRT3 enhancement downregulates p-mTOR and upregulates p-AMPK to facilitate autophagy in the kidneys of septic AKI mice [77]. Dexmedetomidine ameliorates LPS-elicited activation of NLRP3 inflammasome by promoting autophagy *via* the AMPK/mTOR signaling in AKI [78]. Here, LPS administration promoted AMPK phosphorylation and inhibited mTOR phosphorylation in murine renal tissues, implying that LPS activates AMPK pathway but restrains mTOR pathway. However, this event was counteracted by silenced HYAL1. From the findings above, we

concluded that deficiency of HYAL1 enhanced autophagy *via* the AMPK/mTOR pathway in AKI induced by LPS.

In conclusion, knockdown of HYAL1 mitigates renal dysfunction and renal endothelial glycocalyx disruption and enhances autophagy in LPS-induced AKI mice, which may be achieved *via* the AMPK/mTOR pathway. However, to further improve the reliability of results in our study, the upstream mechanisms of HYAL1 as well as other potential signaling pathways associated with how HYAL1 mediates renal function and endothelial glycocalyx barrier integrity remain to be investigated in the future.

Disclosure statement

Funding

References

[1] Uhle F, Lichtenstern C, Brenner T, et al. [Pathophysiology of sepsis]. Anasthesiol Intensivmed Notfallmed Schmerzther. 2015;50(2):114–122.

[2] Plotnikov EY, Brezgunova AA, Pevzner IB, et al. Mechanisms of LPS-Induced acute kidney injury in neonatal and adult rats. Antioxidants. 2018;7(8):105.

[3] Gatward JJ, Gibbon GJ, Wrathall G, et al. Renal replacement therapy for acute renal failure: a survey of practice in adult intensive care units in the United Kingdom. Anaesthesia. 2008;63(9):959–966.

[4] Wu Y, Zhang Y, Wang L, et al. The role of autophagy in kidney inflammatory injury via the NF-κB route induced by LPS. Int J Med Sci. 2015;12(8):655–667.

[5] Shen M, Wang S, Wen X, et al. Dexmedetomidine exerts neuroprotective effect via the activation of the PI3K/Akt/mTOR signaling pathway in rats with traumatic brain injury. Biomed Pharmacother. 2017;95: 885–893.

[6] Feng F, Chen A, Huang J, et al. Long noncoding RNA SNHG16 contributes to the development of bladder cancer via regulating miR-98/STAT3/Wnt/β-catenin pathway axis. J Cell Biochem. 2018;119(11):9408–9418.

[7] Doi K, Leelahavanichkul A, Yuen PS, et al. Animal models of sepsis and sepsis-induced kidney injury. J Clin Invest. 2009;119(10):2868–2878.

[8] Tarbell JM, Cancel LM. The glycocalyx and its significance in human medicine. J Intern Med. 2016;280(1): 97–113.

[9] Reitsma S, Slaaf DW, Vink H, et al. The endothelial glycocalyx: composition, functions, and visualization. Pflugers Arch. 2007;454(3):345–359.

[10] Diebel ME, Martin JV, Liberati DM, et al. The temporal response and mechanism of action of tranexamic acid in endothelial glycocalyx degradation. J Trauma Acute Care Surg. 2018;84(1):75–80.

[11] Chelazzi C, Villa G, Mancinelli P, et al. Glycocalyx and sepsis-induced alterations in vascular permeability. Crit Care. 2015;19(1):26.

[12] Inkinen N, Pettilä V, Lakkisto P, et al. Association of endothelial and glycocalyx injury biomarkers with fluid administration, development of acute kidney injury, and 90-day mortality: data from the FINNAKI observational study. Ann Intensive Care. 2019;9(1):103.

[13] Ushiyama A, Kataoka H, Iijima T. Glycocalyx and its involvement in clinical pathophysiologies. J Intensive Care. 2016;4(1):59.

[14] Nordling S, Hong J, Fromell K, et al. Vascular repair utilising immobilised heparin conjugate for protection against early activation of inflammation and coagulation. Thromb Haemost. 2015;113(6):1312–1322.

[15] Liu HQ, Li J, Xuan CL, et al. A review on the physiological and pathophysiological role of endothelial glycocalyx. J Biochem Mol Toxicol. 2020;34(11):e22571.

[16] Kobayashi T, Chanmee T, Itano N. Hyaluronan: metabolism and function. Biomolecules. 2020;10(11):1525.

[17] Abbruzzese F, Basoli F, Costantini M, et al. Hyaluronan: an overview. J Biol Regul Homeost Agents. 2017;31(4 Suppl 2):9–22.

[18] Rügheimer L, Johnsson C, Maric C, et al. Hormonal regulation of renomedullary hyaluronan. Acta Physiol. 2008;193(2):191–198.

[19] Göransson V, Hansell P, Moss S, et al. Renomedullary interstitial cells in culture; the osmolality and oxygen tension influence the extracellular amounts of hyaluronan and cellular expression of CD44. Matrix Biol. 2001;20(2):129–136.

[20] Khan N, Niazi ZR, Rehman FU, et al. Hyaluronidases: a therapeutic enzyme. Protein Pept Lett. 2018;25(7): 663–676.

[21] Velesiotis C, Vasileiou S, Vynios DH. Analyzing hyaluronidases in biological fluids. Methods Mol Biol. 2019; 1952:127–142.

[22] Colombaro V, Jadot I, Declèves AE, et al. Lack of hyaluronidases exacerbates renal post-ischemic injury, inflammation, and fibrosis. Kidney Int. 2015;88(1):61–71.

[23] Lenoir O, Tharaux PL, Huber TB. Autophagy in kidney disease and aging: lessons from rodent models. Kidney Int. 2016;90(5):950–964.

[24] Wang P, Shao B-Z, Deng Z, et al. Autophagy in ischemic stroke. Prog Neurobiol. 2018;163-164:98–117.

[25] Han D, Jiang L, Gu X, et al. SIRT3 deficiency is resistant to autophagy-dependent ferroptosis by inhibiting the AMPK/mTOR pathway and promoting GPX4 levels. J Cell Physiol. 2020;235(11):8839–8851.

[26] Liu Z, Liu H, Xiao L, et al. STC-1 ameliorates renal injury in diabetic nephropathy by inhibiting the expression of BNIP3 through the AMPK/SIRT3 pathway. Lab Invest. 2019;99(5):684–697.

[27] Bao H, Zhang Q, Liu X, et al. Lithium targeting of AMPK protects against cisplatin-induced acute kidney injury by enhancing autophagy in renal proximal

tubular epithelial cells. FASEB J. 2019;33(12):14370–14381.

[28]　Allouch S, Munusamy S. Metformin attenuates albumin-induced alterations in renal tubular cells in vitro. J Cell Physiol. 2017;232(12):3652–3663.

[29]　Wang Z, Wu J, Hu Z, et al. Dexmedetomidine alleviates lipopolysaccharide-Induced acute kidney injury by inhibiting p75NTR-mediated oxidative stress and apoptosis. Oxid Med Cell Longev. 2020;2020:5454210.

[30]　Lv LL, Wang C, Li ZL, et al. SAP130 released by damaged tubule drives necroinflammation via miRNA-219c/mincle signaling in acute kidney injury. Cell Death Dis. 2021;12(10):866.

[31]　Kim JY, Leem J, Hong HL. Melittin ameliorates Endotoxin-Induced acute kidney injury by inhibiting inflammation, oxidative stress, and cell death in mice. Oxid Med Cell Longev. 2021. 2021;2021:8843051.

[32]　Rocha DJ, Santos CS, Pacheco LG. Bacterial reference genes for gene expression studies by RT-qPCR: survey and analysis. Antonie Van Leeuwenhoek. 2015;108(3):685–693.

[33]　Xie Z, Wei L, Chen J, et al. Calcium dobesilate alleviates renal dysfunction and inflammation by targeting nuclear factor kappa B (NF-κB) signaling in sepsis-associated acute kidney injury. Bioengineered. 2022;13(2):2816–2826.

[34]　Chen YT, Sun CK, Lin YC, et al. Adipose-derived mesenchymal stem cell protects kidneys against ischemia-reperfusion injury through suppressing oxidative stress and inflammatory reaction. J Transl Med. 2011;9:51.

[35]　Kyrylkova K, Kyryachenko S, Leid M, et al. Detection of apoptosis by TUNEL assay. Methods Mol Biol. 2012;887:41–47.

[36]　Fan Z, Cai L, Wang S, et al. Baicalin prevents myocardial ischemia/reperfusion injury through inhibiting ACSL4 mediated ferroptosis. Front Pharmacol. 2021;12:628988.

[37]　Wang J, Chen Y, Tang Z, et al. LncRNA NEAT1 regulated inflammation and apoptosis in a rat model of sepsis-induced acute kidney injury via MiR-27a-3p/TAB3 axis. Biosci Biotechnol Biochem. 2020;84(11):2215–2227.

[38]　Teo SH, Endre ZH. Biomarkers in acute kidney injury (AKI). Best Pract Res Clin Anaesthesiol. 2017;31(3):331–344.

[39]　Chen Y, Luan L, Wang C, et al. Dexmedetomidine protects against lipopolysaccharide-induced early acute kidney injury by inhibiting the iNOS/NO signaling pathway in rats. Nitric Oxide. 2019;85:1–9.

[40]　Abassi Z, Goligorsky MS. Heparanase in acute kidney injury. Adv Exp Med Biol. 2020;1221:685–702.

[41]　Wu F, Wang JY, Chao W, et al. miR-19b targets pulmonary endothelial syndecan-1 following hemorrhagic shock. Sci Rep. 2020;10(1):15811.

[42]　Sun J, Zhang J, Tian J, et al. Mitochondria in sepsis-induced AKI. J Am Soc Nephrol. 2019;30(7):1151–1161.

[43]　Gómez H, Kellum JA. Sepsis-induced acute kidney injury. Curr Opin Crit Care. 2016;22(6):546–553.

[44]　Liu R, Wang SC, Li M, et al. An inhibitor of DRP1 (Mdivi-1) alleviates LPS-induced septic AKI by inhibiting NLRP3 inflammasome activation. Biomed Res Int. 2020;2020:2398420.

[45]　Ferrè S, Deng Y, Huen SC, et al. Renal tubular cell spliced X-box binding protein 1 (Xbp1s) has a unique role in sepsis-induced acute kidney injury and inflammation. Kidney Int. 2019;96(6):1359–1373.

[46]　Leng D, Huang X, Yi J, et al. HYAL1 is downregulated in idiopathic pulmonary fibrosis and inhibits HFL-1 fibroblast proliferation when upregulated. Biomed Res Int. 2020. 2020:3659451.

[47]　Anand D, Ray S, Srivastava LM, et al. Evolution of serum hyaluronan and syndecan levels in prognosis of sepsis patients. Clin Biochem. 2016;49(10-11):768–776.

[48]　Garantziotis S, Savani RC. Hyaluronan biology: a complex balancing act of structure, function, location and context. Matrix Biol. 2019;78-79:1–10.

[49]　Campo GM, Avenoso A, Micali A, et al. High-molecular weight hyaluronan reduced renal PKC activation in genetically diabetic mice. Biochim Biophys Acta. 2010;1802(11):1118–1130.

[50]　Wells A, Larsson E, Fellström B, et al. Role of hyaluronan in chronic and acutely rejecting kidneys. Transplant Proc. 1993;25(2):2048–2049.

[51]　Declèves AE, Caron N, Nonclercq D, et al. Dynamics of hyaluronan, CD44, and inflammatory cells in the rat kidney after ischemia/reperfusion injury. Int J Mol Med. 2006;18(1):83–94.

[52]　Kong T, Zhang SH, Zhang C, et al. The effects of 50 nm unmodified nano-ZnO on lipid metabolism and semen quality in male mice. Biol Trace Elem Res. 2020;194(2):432–442.

[53]　Han B, Li S, Lv Y, et al. Dietary melatonin attenuates chromium-induced lung injury via activating the Sirt1/pgc-1α/Nrf2 pathway. Food Funct. 2019;10(9):5555–5565.

[54]　Hao M, Liu R. Molecular mechanism of CAT and SOD activity change under MPA-CdTe quantum dots induced oxidative stress in the mouse primary hepatocytes. Spectrochim Acta A Mol Biomol Spectrosc. 2019;220:117104.

[55]　Li L, Liu X, Li S, et al. Tetrahydrocurcumin protects against sepsis-induced acute kidney injury via the SIRT1 pathway. Ren Fail. 2021;43(1):1028–1040.

[56]　Sahu BD, Kumar JM, Sistla R. Baicalein, a bioflavonoid, prevents cisplatin-induced acute kidney injury by up-regulating antioxidant defenses and down-regulating the MAPKs and NF-κB pathways. PLoS One. 2015;10(7):e0134139.

[57]　Ben-Mahdi MH, Dang PM-C, Gougerot-Pocidalo M-A, et al. Xanthine oxidase-derived ROS display a biphasic effect on endothelial cells adhesion and FAK phosphorylation. Oxid Med Cell Longev. 2016;2016:9346242.

[58]　Chen TH, Liao FT, Yang YC, et al. Inhibition of inducible nitric oxide synthase ameliorates myocardial ischemia/reperfusion injury - induced acute renal injury. Transplant Proc. 2014;46(4):1123–1126.

[59]　Wang P, Zhu Q, Wu N, et al. Tyrosol attenuates ischemia-reperfusion-induced kidney injury via inhibition of inducible nitric oxide synthase. J Agric Food Chem. 2013;61(15):3669–3675.

[60] Shimokawa T, Yoneda K, Yamagata M, et al. Yohimbine ameliorates lipopolysaccharide-induced acute kidney injury in rats. Eur J Pharmacol. 2020;871: 172917.

[61] Indo HP, Davidson M, Yen HC, et al. Evidence of ROS generation by mitochondria in cells with impaired electron transport chain and mitochondrial DNA damage. Mitochondrion. 2007;7(1-2):106–118.

[62] Song G, Wang RL, Chen ZY, et al. Toxic effects of sodium fluoride on cell proliferation and apoptosis of Leydig cells from young mice. J Physiol Biochem. 2014;70(3):761–768.

[63] Yang X, Fang Y, Hou J, et al. The heart as a target for deltamethrin toxicity: inhibition of Nrf2/HO-1 pathway induces oxidative stress and results in inflammation and apoptosis. Chemosphere. 2022;300:134479.

[64] Pillinger NL, Kam P. Endothelial glycocalyx: basic science and clinical implications. Anaesth Intensive Care. 2017;45(3):295–307.

[65] Jedlicka J, Becker BF, Chappell D. Endothelial glycocalyx. Crit Care Clin. 2020;36(2):217–232.

[66] Abassi Z, Armaly Z, Heyman SN. Glycocalyx degradation in ischemia-reperfusion injury. Am J Pathol. 2020;190(4):752–767.

[67] Lipowsky HH. The endothelial glycocalyx as a barrier to leukocyte adhesion and its mediation by extracellular proteases. Ann Biomed Eng. 2012;40(4):840–848.

[68] Onorati AV, Dyczynski M, Ojha R, et al. Targeting autophagy in cancer. Cancer. 2018;124(16):3307–3318.

[69] Zhao J, Zheng H, Sui Z, et al. Ursolic acid exhibits anti-inflammatory effects through blocking TLR4-MyD88 pathway mediated by autophagy. Cytokine. 2019;123:154726.

[70] Tanida I, Ueno T, Kominami E. LC3 and autophagy. Methods Mol Biol. 2008;445:77–88.

[71] Chen S, Rehman SK, Zhang W, et al. Autophagy is a therapeutic target in anticancer drug resistance. Biochim Biophys Acta. 2010;1806(2):220–229.

[72] Lamark T, Svenning S, Johansen T. Regulation of selective autophagy: the p62/SQSTM1 paradigm. Essays Biochem. 2017;61(6):609–624.

[73] Jiang T, Harder B, Rojo de la Vega M, et al. p62 links autophagy and Nrf2 signaling. Free Radic Biol Med. 2015;88(Pt B):199–204.

[74] Vasko R, Ratliff BB, Bohr S, et al. Endothelial peroxisomal dysfunction and impaired pexophagy promotes oxidative damage in lipopolysaccharide-induced acute kidney injury. Antioxid Redox Signal. 2013;19(3):211–230.

[75] Wang Y, Zhang H. Regulation of autophagy by mTOR signaling pathway. Adv Exp Med Biol. 2019;1206:67–83.

[76] Kim J, Kundu M, Viollet B, et al. AMPK and mTOR regulate autophagy through direct phosphorylation of Ulk1. Nat Cell Biol. 2011;13(2):132–141.

[77] Zhao W, Zhang L, Chen R, et al. SIRT3 protects against acute kidney injury via AMPK/mTOR-Regulated autophagy. Front Physiol. 2018;9:1526.

[78] Yang T, Feng X, Zhao Y, et al. Dexmedetomidine enhances autophagy via α2-AR/AMPK/mTOR pathway to inhibit the activation of NLRP3 inflammasome and subsequently alleviates lipopolysaccharide-induced acute kidney injury. Front Pharmacol. 2020;11:790.